Nanoenergetic Materials for MEMS: A Review

Carole Rossi, Kaili Zhang, Daniel Estève, Pierre Alphonse,
Philippe Tailhades, and Constantin Vahlas

***Abstract*—New energetic materials (EMs) are the key to great advances in microscale energy-demanding systems as actuation part, igniter, propulsion unit, and power. Nanoscale EMs (nEMs) particularly offer the promise of much higher energy densities, faster rate of energy release, greater stability, and more security (sensitivity to unwanted initiation). nEMs could therefore give response to microenergetics challenges. This paper provides a comprehensive review of current research activities in nEMs for microenergetics application. While thermodynamic calculations of flame temperature and reaction enthalpies are tools to choose desirable EMs, they are not sufficient for the choice of good material for microscale application where thermal losses are very penalizing. A strategy to select nEM is therefore proposed based on an analysis of the material diffusivity and heat of reaction. Finally, after a description of the different nEMs synthesis approaches, some guidelines for future investigations are provided. [2006-0259]**

***Index Terms*—Materials processing, materials science and technology, microelectromechanical devices, microelectromechanical system (MEMS), micropyrotechnics, nanoscale energetic materials (nEMs), propulsion, synthesis, thermal power generation.**

I. Introduction

ENERGETIC materials (EMs) are substances that store chemical energy. Conventional EMs can be classified into different classes, i.e., propellants, explosives, and pyrotechnics. Propellants and pyrotechnics release their energy through relatively slow deflagration processes that last for several seconds (combustion). Explosives release their energy in fast detonation processes (microsecond timescale). Basically, traditional EMs are produced by the following.

1) The mixing of oxidizer and fuel constituents into one molecule to produce monomolecular EMs (for example, nitrocellulose, nitroglycerine, and trinitrotoluene).
2) The mixing of oxidizer powders (potassium or ammonium nitrate or perchlorate, ...) and fuel powders (carbon, sulfur, ...) to produce composite EMs (black powder for example). These composites exhibit high energy density, but their energy release rates are slower than monomolecular material because the mass transport rate is limited by the granulometry of the reactants.

Manuscript received November 19, 2006; revised January 12, 2007. Subject Editor S. M. Spearing.

C. Rossi, K. Zhang, and D. Estève are with Microsystems and Systems Integration (MIS), Laboratoire d'Analyse et d'Architecture des Systèmes (LAAS)–Centre National de la Recherche Scientifique, 31077 Toulouse Cedex 4, France (e-mail: rossi@laas.fr; kaili_zhang@hotmail.com).

P. Alphonse, P. Tailhades, and C. Vahlas are with Centre Interuniversitaire de Recherche et d'Ingénierie des Matériaux (CIRIMAT), 31062 Toulouse Cedex 4, France (e-mail: alphonse@chimie.ups-tlse.fr; chane@chimie.ups-tlse.fr; tailhade@chimie.ups-tlse.fr; constantin.vahlas@ensiacet.fr).

Color versions of one or more of the figures in this paper are available online at http://ieeexplore.ieee.org.

Digital Object Identifier 10.1109/JMEMS.2007.893519

Traditional EMs (monomolecular or composite) are relatively easy to prepare (by mixing), and their performances can be predicted and tailored by adjusting the stoichiometry of the chemical reactants. For years, they have been widely used in military, mining, and demolition applications. For two decades, EMs have drawn a growing interest in the scientific community and civil industry since they are very attractive sources of onboard energy to generate gas, heat, and power. Typically, the combustion of propellant produces 5 MJ/kg, while a modern chemical lithium battery used in new laptops only stores 0.5 MJ/kg. Therefore, EMs could have a major impact on microenergetic field. Applications include microthrust [1]–[10], microinitiation [11]–[15], gases for actuation (including injection or moving fluid) [16]–[20], gases for chemical reaction [21]–[24], heating (power) and welding [25], and switching [26]. Various teams have successfully investigated chemical and technological ways to tailor EMs to the targeted applications either to produce gas, heat, or chemical compound. An important challenge that is not really addressed is the compatibility of the EMs with MEMS technologies. This implies two exigencies. First, the thin film of EMs must be grown or deposited at low temperature (below 250 °C). For some applications for which the EMs film is deposited in freestanding microstructures, its stress has to be controlled without any heat treatments. Some well-known semiconductor processing technique such as PVD followed by liftoff [27], [28], screen printing [1], or chemical reaction [13] have been already investigated to prepare and deposit EMs on silicon surface. The second exigency is to minimize heat losses which is one of the most challenging issues to be solved in MEMS applications.

Despite the significant improvements that have been performed through chemical formulation by combining known chemical compounds/molecules [29], the traditional composite and monomolecular EMs feature a relatively slow reaction rate for microscale applications [30]. For example, HMX deflagration will quench in steel tubes of several millimeters in diameter at atmospheric pressure. GAP/AP combustion will quench in glass tubes of 1.4 mm in diameter at atmospheric pressure [31]. To satisfy energy demanding systems of micrometer size, more reactive EMs than traditional ones are required. Significant efforts have been made to introduce metal powder with micro and nanosized particles into traditional EMs. Faster combustion velocities have been demonstrated [32]–[34]. However, difficulties in handling such powders and their incorporation into existing formulations have also been reported. Besides traditional EMs, inorganic energetic composite combining metal oxidizer and metal also called metastable intermolecular composite (MIC) are good candidates as well. They undergo a solid-state redox reaction that is rapid and very

exothermic (nearly twice that of the best monomolecular EM). First results demonstrated mainly empirically that the initiation and combustion properties of EMs are strongly influenced by their microscopical properties. They suggest that reducing the particle size to the nanoscale may result in reduction of the mass-transport rate and therefore would increase the burning rates making these nanoscale EMs (nEMs) attractive alternatives to monomolecular structures.

This paper presents a review of nEMs, a young but very active field of research. To begin, we introduce the recently synthesized nEMs and give the main performance reported by the authors. A section is dedicated to MIC: it is an important class of materials that combine excellent performances with interesting synthetic approaches for MEMS compatibility. While thermodynamic calculations of adiabatic flame temperature and reaction enthalpies are tools to help the choice of desirable EMs, they are not sufficient, in general, for the choice of good material for microscale application where thermal losses have to be taken into account. Section IV will discuss design considerations for nEMs for pyrotechnic systems of micrometer size. Section V will review the different approaches to the synthesis of nEMs. An analysis of the compatibility of the different synthesis routes with MEMS will be given. Lastly, some guidelines for future investigations are provided in the conclusions.

A list of abbreviations used in the review paper is given in Table I.

TABLE I
ACRONYMS, ABBREVIATIONS, AND NOMENCLATURE

AFM	Atomic Force Microscope
ALD	Atomic Layer Deposition
AN	Ammonium Nitrate (NH_4NO_3)
AP	Ammonium Perchlorate (NH_4ClO_4)
CNT	Carbon Nanotube
CVD	Chemical Vapor Deposition
EM	Energetic Materials
GAP	Glycidyl Azide Polymer
HMX	Cyclotetramethylene-tetranitramine ($C_4H_8N_8O_8$)
HTPB	Hydroxyl-terminated Polybutadiene
MEMS	Microelectromechanical Systems
MIC	Metastable Intermolecular Composite
MO	Metal Oxide
PETN	Pentaerythritol Tetranitrate ($C_5H_8N_4O_{12}$)
PSi	Porous Silicon
PVD	Physical Vapor Deposition
RDX	Cyclotrimethylenetrinitramine ($C_3H_6N_6O_6$)
SEM	Scanning Electron Microscopy
TEM	Transmission Electron Microscopy
VD	Vapor Depostion
ZPP	Zirconium Perchlorate Potassium
α	Diffusivity (cm^2/s)
Cp	Heat Capacity (J/kgK)
d	Particle Diameter (m)
k	Thermal Conductivity (W/mK)
m	Mass (kg)
ρ	Density (kg/m^3)
r	Combustion Rate (mm^2/s)
t	Time (s)
T_{ad}	Adiabatic Reaction Temperature (K)
ΔH	Heat of Reaction (cal/g)

II. REVIEW OF EMS FOR MICROSCALE APPLICATION

The first route explored by researchers was to adapt traditional EMs to microscale combustion by incorporating nanoparticles of Al into traditional propellants or explosives. Doping composite propellant with thermal conductive nanoscale particles has demonstrated a slight enhancement in the reactivity of the mixture [31], [35]. Then, with the progress of nanoengineering, researchers preferred to combine or synthesize inorganic energetic nanocomposite composed of particles of oxidizer (typically metal oxide) and fuel (mainly Al) to produce MIC.

A. Nanoparticle-Doped Propellant

Nano-Al is the most widely used metallic doping particle for the following reasons.

1) Al is a common metal used in technology and is relatively low cost.
2) The formation of a thin oxide layer around each Al particle prevents Al powder from spontaneous combustion [33], [36].
3) Al can be easily produced in nanoparticles form (50–120 nm) and nano-Al is commercially available for example from NovaCentrix, formerly known as Nanotechnologies, Inc.
4) Al enhances the reactive power of the material by increasing the combustion velocity due to its high thermal conductivity.

In 1997, Brown *et al.* [34] investigated the influence of the incorporation of microsized Sb particles into $KMnO_4$ and found that reducing particle size from 14 to 2 μm increased the burning rate by a factor of 4. Ivanov and Tepper [37] reported that by adding aluminium nanoparticles in a propellant formulation, the mixture burning rate could be enhanced by a factor of 5–10. Chiaverini *et al.* [38] demonstrated an increase of 70% in burning rate of HTPB-based solid propellant doped with 20% of nanoparticles of Al. Armstrong *et al.* [39] confirmed that the burning rate of the AP-based propellants increases when conventional Al powder is replaced by nano-Al. The burning rate increases from 1 to more than 100 mm/s when the aluminum particle size decreases from 10 μm to 100 nm. This tendency has been confirmed for several types of propellants (HTPB/AP, GAP/AP, and GAP/AN) by numerous authors and studies [31], [40]–[43]. The ignition time is also reduced when the propellant is doped with Al nanoparticles [41]. However, for explosives, the use of metallic nanopowder has not proven to be effective [43].

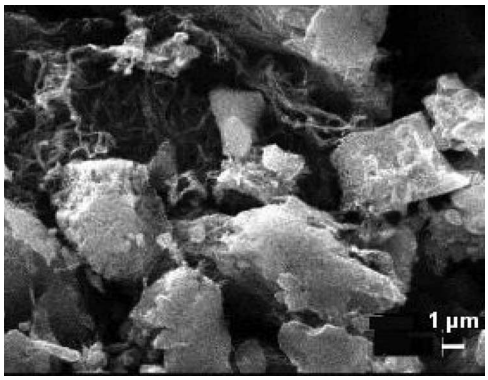

Fig. 1. SEM image of micrometer-sized PETN grains among CNTs. Reproduced with permission from [44]. Copyright 2005 American Chemical Society.

In conclusion, doping propellant with Al nanoparticles improves slightly its reactivity and ignition capability; the maximum burning enhancement seems to be reached when the Al content represents 20% of the propellant mass. However, recent studies reveal that the incorporation of nanosized metal particles into propellants does not increase the reaction temperature and burning rate sufficiently to compensate the thermal losses occurring in microscale devices. These nano-Al doped propellants suit mesoscale applications but are not applicable for microscale applications. The quenching diameter is around the millimeter, and the combustion is unstable in the centimeter scale. Furthermore, some authors have reported [40] that an AP-based propellant with pure nano-Al has unstable and nonreproducible combustion because of the difficulty to uniformly mix the ultrafine Al particles into the propellant. Other approaches have been therefore considered. One is the incorporation of carbon nanotubes (CNT), having very high thermal conductivity, into traditional propellant, and the other is developed by Pivkina *et al.* to produce nanopowder of AN and RDX. Very recently, Manaa *et al.* [44] presented a study of ignition and combustion of explosive-nanotube mixture. They incorporated single-wall CNT produced by Carbon Nanotechnologies, Inc. inside a PETN EM and demonstrated that the mixture (see Fig. 1) can burn rapidly with local temperature estimated between 1500 °C–2000 °C. Shock wave with an average speed of 6.8 km/s has been measured.

According to the authors, in a longer term, there is hope that CNTs could be used to encapsulate energetic ingredients/molecules to produce an EM that not only has good energetic performance but also has much improved handling and long-term storage capabilities.

An interesting vacuum codeposition technique was presented by Pivkina *et al.* to synthesize nanostructured AN, RDX, and AN/RDX composites [4], [45]. The typical process of synthesizing nano-RDX and AN/RDX consists of realizing nanopowder of the constituent (AN, RDX) by vacuum condensation of evaporated pure bulk substrates onto the cooled substrates to obtain AN and RDX powder with 50 nm in diameter. Conventional AN and RDX powder with 200 and 50 μm in diameter, respectively, have been compared with nano-AN and RDX powder with 50 nm in diameter. According to the results, the burning rate can be doubled for nanoscale RDX: 15.1 mm/s for the conventional RDX and 30 mm/s for the nanoscale one. Pure AN could not have a sustained combustion; only thermal analysis has been performed and showed that the temperature of maximun heat release for AN nanopowder is less than that for conventional one. Vasylkiv *et al.* [23], [24] proposed nanoreactors produced by nanoblasts impregnated with particles of $C_3H_6N_6O_6$. The described technique opens the door to the synthesis of a wide range of multimetal oxide ceramic and metal-ceramic composite nanopowders with precise stoichiometries and uniform morphologies.

B. Nanoscale Thermite Material or MIC

Thermite reaction is a highly exothermic reaction that involves a metal reacting with a metallic or a nonmetallic oxide to form a stable oxide and the corresponding metal or nonmetal of the reactant oxide [46]. This is a form of oxidation–reduction reaction that can be written as

$$\mathrm{M} + \mathrm{AO} \rightarrow \mathrm{MO} + \mathrm{A} + \Delta H$$

where M is a metal or an alloy, A is either a metal or a nonmetal, MO and AO are their corresponding oxides, and ΔH is the heat of reaction. The thermite reactions exhibit fast reaction rates that make their use extremely energy efficient.

Nano-Al is most widely used as the fuel for the reasons detailed in Section II-A plus additional advantages for thermite reactions.

1) Al has low vapor pressure: Al, unlike calcium or magnesium, does not require a pressure-tight reaction vessel for the reaction.
2) Al melting temperature is low (approximately 660 °C) resulting in a low ignition temperature.

Among a large number of possible oxidizers [52], only a few have been investigated by different teams: Fe_2O_3, MoO_3, $KMnO_4$, CuO, NiO, MnO_2, WO_3, SnO_2, and SiO_2.

In 1995, Aumann *et al.* [33] produced MoO_3/Al MIC being 20–50 nm in diameter. When the mixture is stoichiometric, the energy density reached 16 kJ/cm^3, and the mixture can burn 1000 times faster than macroscale thermite material. Bockmon *et al.* [47] compared different samples of Al/MoO_3 MIC fabricated using ultrasonic mixing where nano-Al was used. The measured average combustion velocity increases from approximately 685 to 990 m/s when the Al particle size is decreased from 121 to 44 nm. As a comparison, micrometer scale Al/MoO_3 burns at 10 mm/s [34]. Authors also note that the reaction rate becomes independent of Al particle diameter below a critical diameter, which is 40 nm in their case. This could be explained by the fact that, when the Al particle diameter decreases, the proportion of Al_2O_3 over Al increases resulting in a reduction of the volume of active material and possible inhibition of the thermite reaction.

Granier and Pantoya [48], [49] observed that the burning rate of nano-Al/MoO_3 MIC is enhanced by a factor of 10 when the average Al particle size decreases from 20 000 to 50 nm. Moreover, they noted that by decreasing the Al particle size from micrometer to nanometer scale in the composite consistently decreases the ignition time by up to two orders of magnitude (from 6 s down to 20 ms) and improves the

repeatability of the composite's response to ignition. The increased sensitivity to ignition may be explained by the reduction in melting temperature associated with nanoparticles. Sun *et al.* [50] studied the reactions of nano-Al with O_2 with the average Al particle diameters ranging from 30 to 160 nm. It was shown that Al/O_2 reacts below the Al melting temperature. The heat released by the reaction (approximately 10 kJ/g) is below the theoretical one (25 kJ/g). Bhattacharya *et al.* [51] investigated the burning rate of nanoscaled CuO/Al and Bi_2O_3/Al. The burning rate reaches the average values of 440 and 150 m/s for nanoscaled CuO/Al and Bi_2O_3/Al, respectively.

Results of empirical studies reported in Section II establish clearly that the initiation temperature, reaction properties, and propagation rate are strongly influenced by the microscopical properties of the EMs, including the size of constituents and intimacy of the contact.

III. Strategy to Design nEMs for Microscale Application

Basically, the synthesis of EMs and the choice of molecules or compounds are mainly guided by molecular modeling and thermochemical codes. This approach has proven its efficiency for traditional EMs and macroscale/mesoscale applications, and significant improvements have been performed through chemical formulation, i.e., combining known chemical compounds/molecules. However, for microscale applications, besides the optimization of energy density given by thermo chemical codes, other considerations have to be taken into account to design novel nEMs.

1) The rate of reaction has to be enhanced to minimize heat losses, not only by increasing the heat of reaction.
2) The technological process has to be controlled to adapt the stoichiometry of reactants, the size of particles, the purity of the final mixture, and the intimacy of the contact between the fuel/oxidizer.
3) The contribution of the mass diffusion rate has to be evaluated since it could limit the combustion rate.

For the first point, we propose a theoretical evaluation that is based on the diffusivity parameter, to guide the selection of any EMs for microscopic application. The second point, which is related to the structural control of the material, is very difficult to be theoretically predicted yet, and it is mainly investigated empirically by numerous research teams. Main results will be presented and discussed in Section IV. For the third point, a simple intuitive reasoning can estimate the scale of the particle size below which diffusion process can be neglected. For that, we consider a spherical particle coated with a thin oxide layer that burns from the external surface to the center, as shown in Fig. 2. The diameter of the particle decreases over the time as follows $\pi \times d^2 = r \times t$ with r as the combustion rate $(\mathrm{mm}^2/\mathrm{s})$, and d as the particle diameter. Therefore, with $r = 1.5\ \mathrm{mm}^2/\mathrm{s}$ (which is the low limit), particles of 100 nm in diameter would be consumed in 0.01 μs. This time is sufficiently short compared to mass diffusion delay[1] to consider the mass diffusion process negligible for particles having diameter lower than 100 nm.

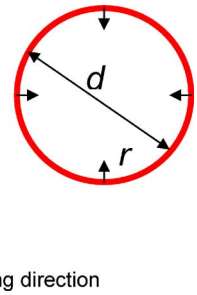

Fig. 2. Schematic of the combustion of a nanoparticle coated with a thin oxide.

For the rest of the section, the mass diffusion phenomena will be neglected, and three parameters will be considered to propose a classification of nEMs: the thermal diffusivity α, the heat of reaction ΔH, and the adiabatic temperature T_{ad}.

1) Diffusivity: $\alpha = k/(\rho \times Cp)$ where k is thermal conductivity, and $\rho \times Cp$ is the volumetric heat capacity. Substances with high thermal diffusivity conduct heat quickly. Tables II and III give the calculated diffusivity for well-known organic EMs and seven thermite EMs: Al/Fe_2O_3, Al/MoO_2, Al/CuO, Al/NiO, Al/SnO_2, Al/SiO_2, and Al/TiO_2.
2) Heat of reaction: for each thermite couple, thermodynamic calculations of heat of reaction (ΔH) and adiabatic flame temperature (T_{ad}) are given in Table IV. The values of T_{ad} are from [52]. For the purpose of comparison, the values of ΔH are from COACH [53], which is an in-house code, and [52], respectively.
3) The adiabatic reaction temperature given in Tables II and IV is the temperature that results from a complete combustion process that occurs without any heat transfer or changes in kinetic or potential energy.

A. Calculation of the Diffusivity of Thermite Materials

We suppose that the aluminum (Al) and metallic oxide (MO)[2] are mixtures of nanoscale powders with d_{Al} and d_{MO} being the Al and MO particle diameter. We also assume that the Al-to-MO mass ratio $(m_{\mathrm{Al}}/m_{\mathrm{MO}})$ is the stoichiometric one for each reaction. The thermal conductivity of Al/MO MIC at 300 K is a function of the diameter of the Al and MO particles as well as thermal conductivities of both Al and MO. In a first approximation, we suppose that the MIC that is composed of Al and MO particles in intimate contact can be modeled as an AL/MO bilayer material. The Al and MO layer thickness would be equal to the Al and MO particle diameter.

The resulting bilayer thermal conductivity can be therefore calculated as the following:

$$k_{\mathrm{Al/MO}} = \frac{k_{\mathrm{Al}} k_{\mathrm{MO}} \times \left(\frac{1}{d_{\mathrm{Al}}} + \frac{1}{d_{\mathrm{MO}}}\right)}{\frac{k_{\mathrm{Al}}}{d_{\mathrm{Al}}} + \frac{k_{\mathrm{MO}}}{d_{\mathrm{MO}}}}$$

[1]Mass diffusion time of a particle of Al of 100 nm in diameter: hundreds of microns.

[2]MO is Fe_2O_3, MoO_2, CuO, NiO, SnO_2, SiO_2, TiO_2.

TABLE II
DIFFUSIVITY, HEAT OF REACTION, AND ADIABATIC TEMPERATURE FOR THREE DIFFERENT ORGANIC EMS

Organic EMs	Diffusivity at 300 K α (cm^2/s)	Heat of reaction ΔH (cal/g)	Adiabatic reaction Temperature T_{ad}(K)
PETN	1.29×10^{-3}	1435	4140
HMX	0.77×10^{-3}	1350	3255
NC	10^{-3}	960	3000

TABLE III
DIFFUSIVITY FOR SEVEN DIFFERENT MICS CALCULATED FOR THREE FUEL-OVER-METALLIC OXIDE DIAMETER RATIOS

MIC	Diffusivity at 300K α (cm^2/s) $d_{Al}=d_{MO}$	Diffusivity at 300K α (cm^2/s) $d_{Al}=0.1\times d_{MO}$	Diffusivity at 300K α (cm2/s) $d_{Al}=10^{-3}\times d_{MO}$
Al/MnO_2	31.64×10^{-3}	17×10^{-3}	16.1×10^{-3}
Al/CuO	60×10^{-3}	33×10^{-3}	30×10^{-3}
Al/Fe_2O_3	85×10^{-3}	49×10^{-3}	45×10^{-3}
Al/NiO	61×10^{-3}	35×10^{-3}	32×10^{-3}
Al/SnO_2	190×10^{-3}	116×10^{-3}	107×10^{-3}
Al/SiO_2	16.5×10^{-3}	9×10^{-3}	8.3×10^{-3}
Al/TiO_2	48.5×10^{-3}	27.3×10^{-3}	25×10^{-3}

TABLE IV
STOICHIOMETRIC MASS RATIO, HEAT OF REACTION (ΔH), AND ADIABATIC TEMPERATURE ($T_{\rm ad}$) FOR SEVEN DIFFERENT MICS

MIC	Stoichiometric mass ratio (Al/MO)	Heat of reaction ΔH (cal/g)		Adiabatic reaction temperature T_{ad} (K)	
		COACH	Ref. [52]	without phase change	with phase change
$4Al + 3MnO_2$	1 / 2.417	1146	1159	4829	2918
2Al + 3CuO	1 / 4.422	987.8	974.1	5718	2843
$2Al + Fe_2O_3$	1 / 2.959	952.0	945.4	4382	3135
2Al + 3NiO	1 / 4.154	855.1	822.3	3968	3187
$4Al + 3SnO_2$	1 / 4.189	686.8	686.8	5019	2876
$4Al + 3SiO_2$	1 / 1.670	515.0	513.3	2010	1889
$Al + TiO_2$	1 / 2.221	379.8	365.1	1955	1752

with $k_{\rm Al}$ and $k_{\rm MO}$ as the thermal conductivities at 300 K of Al and MO, respectively, and $d_{\rm Al}$ and $d_{\rm MO}$ as the diameters of Al and MO particles, respectively.

The heat capacity at 300 K of Al/MO can be calculated as the following:

$$Cp_{\rm Al/MO} = \frac{m_{\rm Al}\times Cp_{\rm Al} + m_{\rm MO}\times Cp_{\rm MO}}{m_{\rm Al}+m_{\rm MO}}$$

with $m_{\rm Al}$ and $m_{\rm MO}$ as the masses of Al and MO contained in the MIC, respectively, and $Cp_{\rm Al}$ and $Cp_{\rm MO}$ as the heat capacitances of Al and MO, respectively.

B. Results and Comments

In Fig. 3, it can be clearly shown that the Al/MO thermite diffusivities decrease when the MO-to-Al particle diameter ratio increases. In consequence for the rest of the study, $d_{\rm Al}$ is taken which is equal to $d_{\rm MO}$.

Fig. 4 classifies the different EMs in a 2-D diagram: heat of reaction in y-axis and diffusivity in x-axis. The graph indicates that any EMs placed in the left bottom corner of the graph could not suit microscale application because of too low heat of reaction and insufficient diffusivity. However, the EMs in the upper right parts of the diagram are considered to be well adapted to MEMS because they release high amount of heat, and the rate is expected to be high. To conclude this short study, among investigated MICs, the best

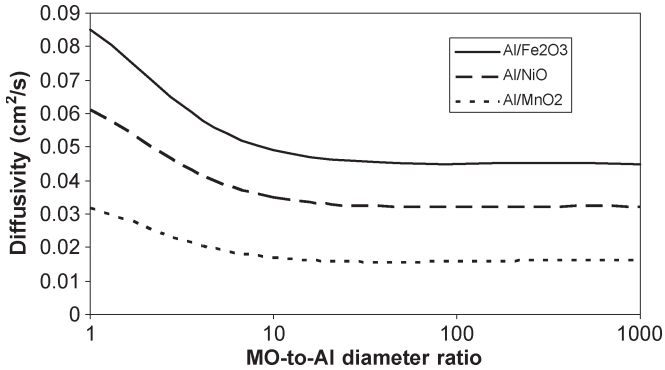

Fig. 3. Example of diffusivity evolution as a function of the MO-to-Al diameter ratio for three MICs: Al/Fe_2O_3, Al/NiO, and Al/MnO_2.

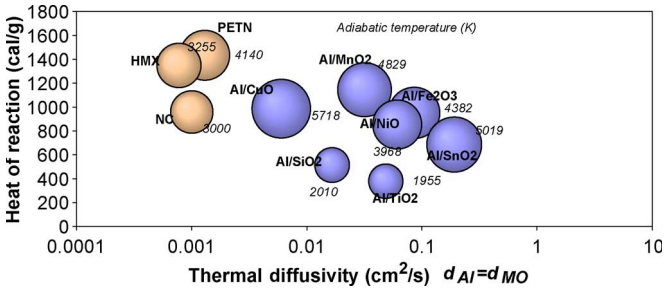

Fig. 4. Classification of EMs in a 2-D diagram (ΔH, α).

ones are: Al/MnO_2, Al/Fe_2O_3, and Al/NiO. From Fig. 4, MICs appear to be a promising category of nEMs that could be a good candidate to realize thin layer of EMs for microscale applications since they have excellent diffusivity, and they can be very reactive compared with traditional organic EMs, and also, they can exhibit high exothermicity. For organic EMs, the best one appears to be PETN that nevertheless presents poor diffusivity.

IV. Synthesis of nEMs for Microscale Applications

There are different approaches to synthesize nanosized thermite composite or MIC. Basically, they can be classified into traditional approaches, which include MEMS compatible approaches, nanopatterning, and "bottom-up" or molecular engineering approaches. In traditional approaches, the nanoparticles of fuel and oxidizer are first synthesized or purchased and then mixed together, i.e., powder mixing. In MEMS compatible approaches, the fuel/oxidizer molecules or particles are synthesized and put together in a single process such as sol–gel chemistry and vapor deposition (VD) techniques. In molecular engineering approaches, the atoms or molecules of fuel and oxidizer are first synthesized and then combined using molecular engineering in solution or via a polymer chain. The "bottom-up" approaches are mainly investigated with the aim at developing a fundamental understanding of the evolution of the EMs properties with the size and intimacy of the constituents. The main synthesis approaches of MIC are presented and discussed in the following.

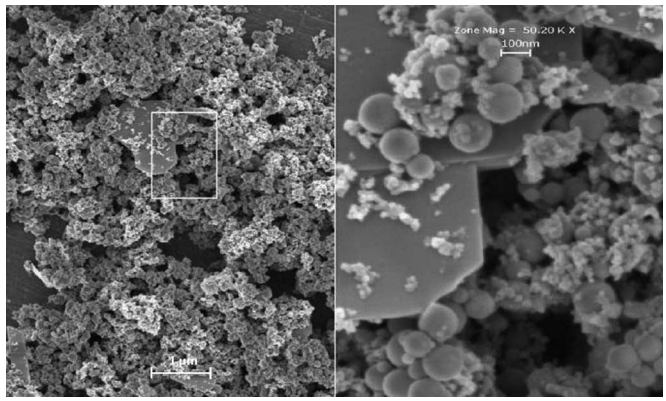

Fig. 5. SEM images of 80-nm Al particles mixed with MoO_3 particles. Reproduced with permission from [48]. Copyright 2004 Elsevier.

A. Powder Mixing

The easiest method is the physical powder mixing. In recent works, the ultrasonic mixing is mostly employed to combine nano-Al and oxidizer powder [40], [47]–[50], [54]–[56]. Typically, the nano-Al and oxidizer are dispersed in solvents (e.g., hexane) and mixed together with ultrasonic wave. The sonication process is used to break up agglomerates and mix both constituents. After sonication, the mixture is heated to evaporate the solvent. The mixture is often passed through a fine mesh to break any agglomerates formed during the evaporation process and produce submicronic powder. Fig. 5 is a representative SEM image of the Al/MoO_3 MIC which, thus, obtained mixture.

Mixing nanopowders of fuel with oxidizer is a simple method. Nevertheless, it presents limitations. First, one is the difficulty to mix intimately ultrafine powder, the second one is the difficulty to obtain a homogeneous distribution of oxidizer and fuel nanoparticles, and thirdly, the manipulation of some powder can be dangerous, and the deposition in thin film or into a microsystem is difficult [30].

B. Sol–Gel/Aerogel Process

A wide variety of glass or glass–ceramic monoliths and nanostructured powders are synthesized through sol–gel technique, since it has the advantages of low temperature processing, high chemical homogeneity, etc. Researchers at Lawrence Livermore National Laboratory have first introduced the use of the sol–gel chemistry to synthesize nEMs [57], [58].

The sol–gel process involves reactions in solution to produce dispersion of nanoparticles in a liquid phase, called "sol" (colloidal solution). By condensation, the sol gives a 3-D solid network, called a "gel," with the open pores being occupied by the solvent. Solvent removal by evaporation produces the collapse of the open pore structure of the gel and leads to a xerogel. Supercritical drying allows removing the solvent without collapsing the gel structure. This leads to a highly porous and lightweight material called aerogel, with excellent uniformity given that the particles and the pores are both in nanoscale. The sol–gel process is illustrated in Fig. 6.

Tillotson *et al.* [58] reported about successful sol–gel synthesis of Fe_2O_3/Al MIC. It consists of clusters of Fe_2O_3

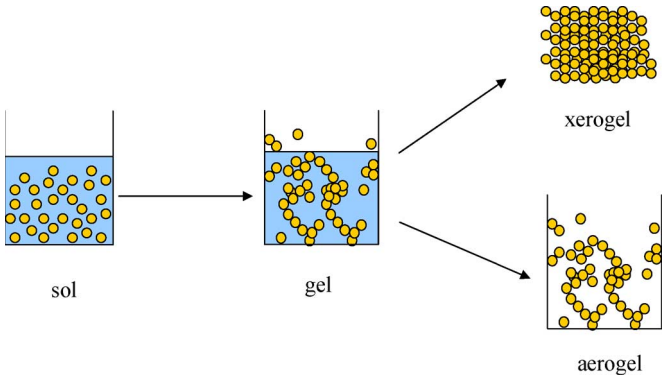

Fig. 6. Schematic diagram of sol–gel methodology.

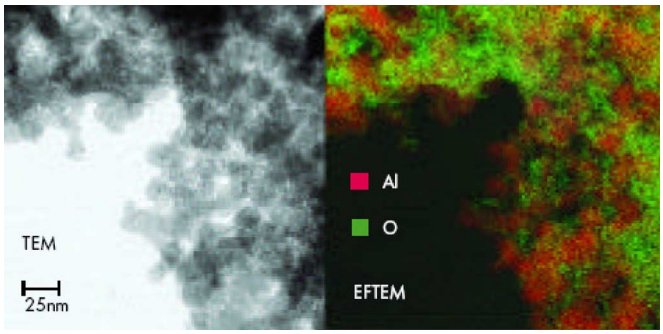

Fig. 7. Al/Fe_2O_3 MIC prepared by sol–gel process. Reproduced with permission from [59]. Copyright 2002 AMMTIAC.

being 3–10 nm in diameter, which are in contact with nano-Al particles of about 30 nm in diameter, as shown in Fig. 7. The obtained specific surface of the Fe_2O_3 nanoporous matrix is around 300–400 m^2/g. The authors proceeded to standard safety tests (spark, friction, ...) showing a relatively insensitivity. Ignition and thermal analysis gave a heat of reaction of 1.5 kJ/g, whereas the theoretical value is 3.9 kJ/g. The authors suggested that the reasons for reduction of the total measured energy could be the substantial passivation of Al powder by a native oxide coating and the presence of organic impurities that could represent 10% in mass of the sample.

The sol–gel chemistry provides process advantages over mixing methods: it is MEMS compatible, low cost, safe, and can potentially produce nEMs with interesting and special properties due to the high porosity. Sol–gel process can also offer good opportunity to tailor the nEMs properties by controlling the process. However, two disadvantages can be noted: First is the random distribution of the particles that can lead to locally a separation between the fuel and oxidizer and, therefore, inhibition of self-sustaining reaction; Second is that sol–gel mixture often has organic impurities that can reach up to 10% of the sample mass leading to a significant reduction of the reaction performance.

Besides the sol–gel chemistry used in [57], [58], and [60], the aero-sol–gel chemistry was also employed to synthesize nano-$KMnO_4$, CuO, Fe_2O_3, and the corresponding MICs with nano-Al as the fuel [55], [61]–[63]. Clapsaddle *et al.* [63], for example, reported that the particle size and properties of the aerogel preparation can be tailored easily by controlling the epoxide addition procedure.

Prakash *et al.* [64] reported a novel aerogel-based process to create a pure nanosized MIC core-shell nanostructure that is obtained by coating a strong oxidizer nanoparticle with a thin layer of relatively mild oxidizer. The authors use a two-temperature aerosol spray-pyrolysis method, as shown in Fig. 8. The core is $KMnO_4$, and the shell is Fe_2O_3. In this process, an aqueous solution of $Fe(NO_3)_3 9H_2O$ and $KMnO_4$ is sprayed into droplets (1 μm in diameter). The environment is dried. The aerosol is then thermal cured. First, it is maintained above the decomposition temperature of iron nitrate (typically 120 °C), and then, the temperature is increased to about 240 °C (approximately melting point of permanganate). The 0.6-μm composite particles are then collected on a filter. At 120 °C, iron nitrate decomposes into Fe_2O_3 enrobing with intimately the solid permanganate. At 240 °C, the permanganate melts, and the Fe_2O_3 aggregates around the $KMnO_4$ particles. The resulting composite nanoparticle of $KMnO_4$ (150 nm in diameter) coated with Fe_2O_3 (4-nm thick) is shown in Fig. 9. Authors performed reactivity experiments and announced that the reactivity can be moderated over a relatively large range by changing the thickness of the iron oxide. Besides the resulting intimate contact between the reactants, the oxide coating thickness on each nanoparticle is nanoscale and could be precisely controlled to lower the ignition temperature and also not to inhibit the thermite reaction.

Prakash's process is interesting to precisely investigate the influence of the nEMs structural properties (oxide thickness for example) on its reactivity. However, it is complex and not currently applicable for mass production process.

C. Vapor Deposition

An alternative route to sol–gel/aerogel chemistry is to deposit alternatively a nanolayer of oxidizer and fuel under vacuum by vapor deposition or sputtering. VD is a chemical process often used in the semiconductor industry for the deposition of thin films of various materials. In a typical VD process, the substrate is exposed to one or more volatile precursors, which react and/or decompose on the substrate surface to produce the desired deposition. Basically, the resulting layer's thickness ranges from 20 nm to 2 μm. Sputtering is a physical process whereby atoms in a solid target material are ejected into the gas phase due to bombardment of the material by energetic ions. It is also commonly used for thin-film deposition.

VD technique has been employed to deposit PETN thin film by Tappan *et al.* [27], [28]. Vine *et al.* [65] reported the VD of Ti/C and Ti/Al multilayers. An increase in the burning rate has been found for multilayered composition compared with the conventional one. Blobaum *et al.* [66] carried out a study on Al/CuO*x* multilayer nanofoils deposited by magnetron sputtering onto silicon substrates. The process of deposition is simple: a CuO target is RF sputtered on silicon in alternance with Al target. To avoid metal interdiffusion, the silicon wafer is cooled down during the deposition process. The deposited compositions exhibit a layered structure Al $(0.3\ \mu\text{m})/Cu_4O_3$ $(0.7\ \mu\text{m})$, as shown in Fig. 10. The measured heat of reaction of the fabricated nanofoils is 3.9 $\pm$ 0.9 kJ/g that is similar to that calculated for the reaction of Al and CuO, as listed in Table IV.

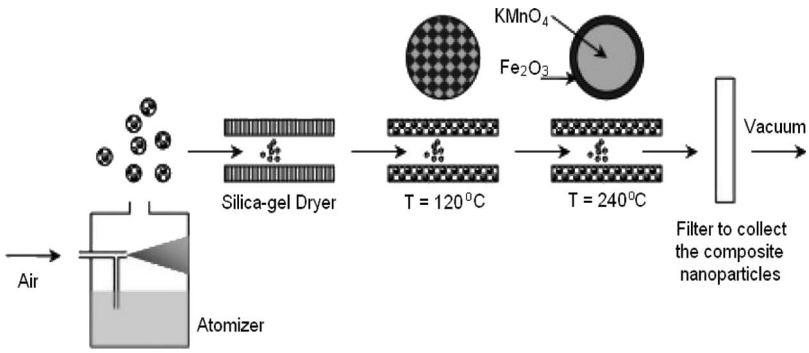

Fig. 8. Aerosol system for the synthesis of core-shell nanocomposite oxidizer. Reproduced with permission from [64]. Copyright 2005 American Chemical Society.

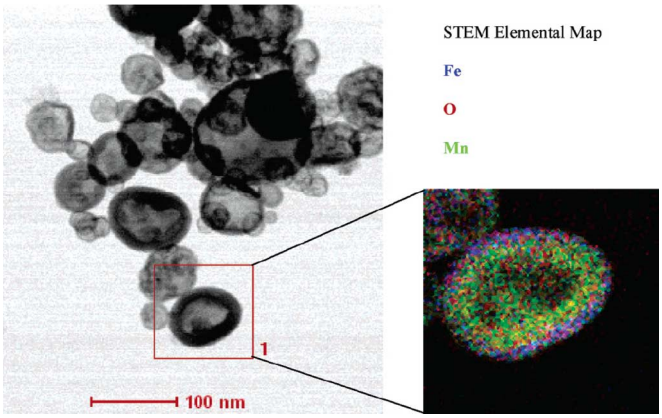

Fig. 9. TEM graph and STEM elemental map of nano-$KMnO_4$ coated with Fe_2O_3. Reproduced with permission from [64]. Copyright 2005 American Chemical Society.

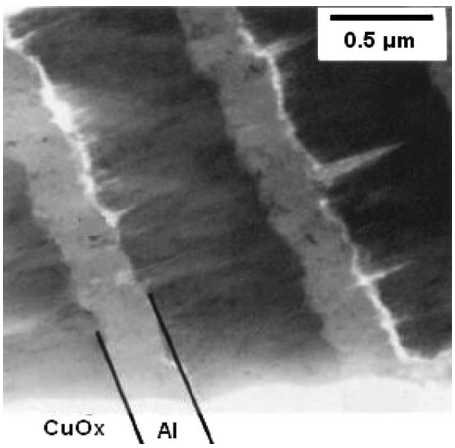

Fig. 10. TEM image of Al/CuOx multilayer nanofoils. Reproduced with permission from [66]. Copyright 2003 American Institute of Physics.

An important dependence of the burning rate with the layer thickness and intermixing conditions has been noticed.

Gavens *et al.* in 1999 [67] has proposed Al/Ni nanofoils deposited using high vacuum dc and RF sputtering. The total thickness of the multilayers foils is 11 μm. Each layer thickness ranges from 12.5 to 200 nm. Then, the foils are annealed to intermix the fuel and the oxidizer by atomic interdiffusion. The rate and heat of reaction are measured for different bilayer thicknesses and intermixing conditions. The 200-nm-thick bilayer has a burning rate of 1 m/s. Authors mention that when the bilayer thickness decreases, the burning rate increases and then drops to zero. For a thick layer (200 nm), the intermixing conditions are negligible, whereas for a thin layer, the reaction rate is controlled by the thickness of the intermixed region.

In a fuel/oxidizer multilayer foil deposited by vapor deposition method, the diffusion distances between fuel and oxidizer are reduced 10–1000 times compared to powders, thereby enhancing atomic mixing and reactivity. The presence of impurities and Al oxidation are much smaller in multilayer foils than in sol–gel or powder mixing process because the foils are deposited in high vacuum.

D. Nanostructuring

1) Atomic Layer Deposition (ALD): Among investigated nanostructuring methods, ALD is an ideal process to deposit ultrathin films with high conformal uniformity and precise thickness control. ALD utilizes sequential precursor gas pulses to deposit a film one layer at a time. ALD has been already utilized to deposit many metal oxides as WO_3 [68], Co_3O_4 [69], and NiO [70]. The maximum thickness is a few tens of nanometers. Ferguson *et al.* [71] employed it to deposit SnO_2 oxidizer coatings on nanoparticles of Al. The Al/SnO_2 MIC prepared by ALD process is shown in Fig. 11. The first experimentations on the Al$-$$SnO_2$ samples show a quick and violent reaction despite the low Sn percent by mass and low Al/O molar ratio.

2) Nanoporous Silicon With Oxidizer: Porous silicon (PSi) has been known as a reactive material when McCord *et al.* [72] discovered a combustion reaction of PSi immersed in nitric acid. The exothermic reactions of PSi with liquid oxygen and gadolinium nitrate were then presented in [73] and [74]. The PSi pores (2–10 nm) are filled with a liquid oxidizer. Because of these findings, PSi-based nEMs were proposed for industrial applications as a component of an airbag initiator [13], [14].

The PSi (Fig. 12) can be produced by electrochemical etching of bulk silicon in solutions containing fluoride (e.g., HF) and H_2O_2 [75]. The porosity and the structure size of the PSi can be adjusted from 2 to 1000 nm by selecting suitable etching parameters such as fluoride concentration, current density, treatment duration, and starting material [14]. The nanopores are then filled with a liquid oxidizer ($Ca(ClO_4)_2$, $KClO_4$, $NaClO_4$, Sulfur, etc.). To enhance the intimacy between

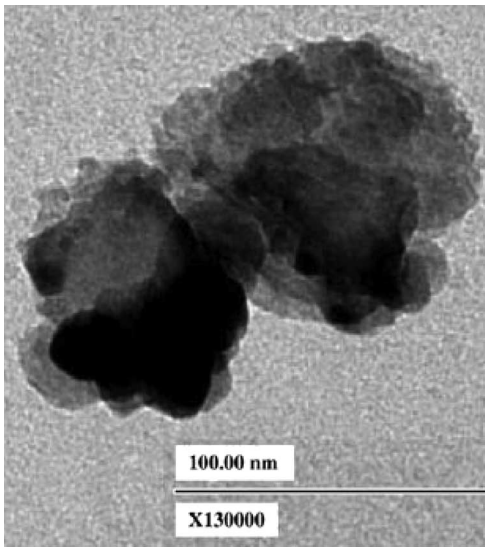

Fig. 11. Al/SnO_2 MIC prepared by ALD process. Reproduced with permission from [71]. Copyright 2005 Elsevier.

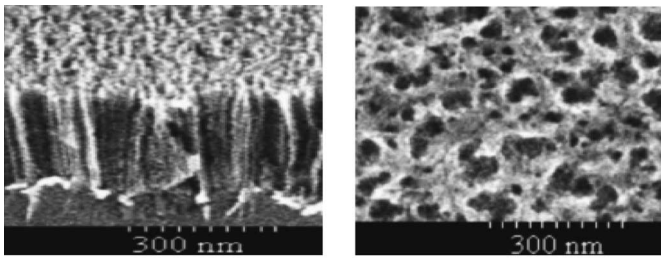

Fig. 12. SEM images of nano-PSi. (a) Cross section. (b) Top view. Reproduced with permission from [75]. Copyright 2000 American Institute of Physics.

the Si and O_2, the PSi matrix can also be filled with the oxidizer by CVD and PVD. The activation energy of the PSi/O_2 reaction can be tailored by controlling the SiO_2 native layer before the oxidizer loading. The results are very promising: Laucht *et al.* [13] tested PSI/$Ca(ClO_4)_2$ and PSI/$Na(ClO_4)_2$ in a calorimetric bomb. Authors noted heats of reaction of 8.6 kJ/g and 9.2 kJ/g for PSI/$Ca(ClO_4)_2$ and PSI/$Na(ClO_4)_2$, respectively, which are well above that of ZPP (6.3 kJ/g).

One particular advantage of PSi-based nEMs is that silicon is one of the base materials for MEMS. Therefore, the nEMs can be conveniently incorporated into silicon-based MEMS devices. This provides the advantage of low cost production and MEMS compatibility. In particular, the PSi-based nEMs can be easily integrated into semiconductor circuitries.

3) Other Approaches: Menon *et al.* [76] realized Al/Fe_2O_3 MIC by embedding an array of Fe_2O_3 nanowires inside a thin Al film, as described in Fig. 13(a). The process started with electrochemical anodization of Al foil to form nanoporous alumina templates [77], [78]. Then, Fe nanowire was fabricated inside the nanopores by electrochemical deposition. After partial etching of the alumina walls from the top, Fe nanowires were revealed and then oxidized. Finally, the remaining alumina walls were etched away, and at this stage, all of the Fe

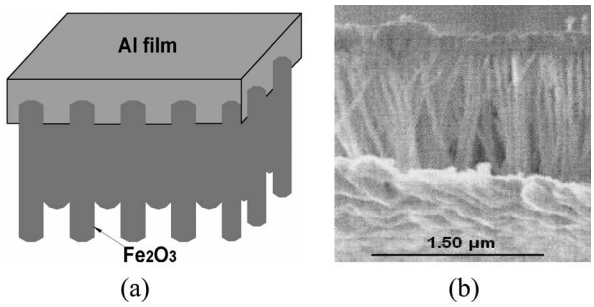

Fig. 13. (a) Schematic of Al/Fe_2O_3 MIC. (b) SEM image of Al/Fe_2O_3 MIC. Reproduced with permission from [76]. Copyright 2004 American Institute of Physics.

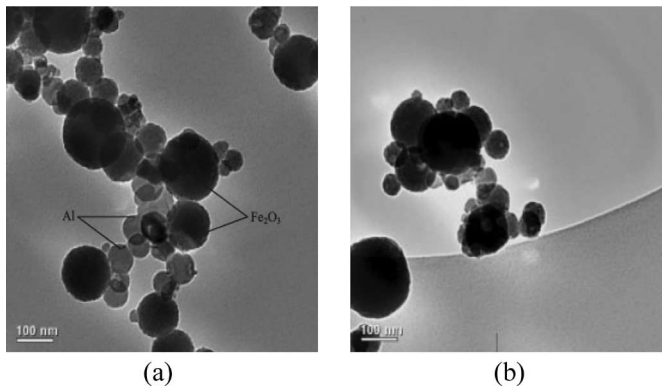

Fig. 14. TEM images of Al/Fe_2O_3 MIC by (a) random assembly and (b) electrostatic assembly. Reproduced with permission from [79]. Copyright 2004 Wiley-VCH Verlag GmbH & Co. KGaA, Weinheim.

nanowires were converted into Fe_2O_3 nanowires by annealing. A typical SEM image of a high-density nanowire array embedded in Al film is shown in Fig. 13(b). The diameter of a single nanowire is about 50 nm, and the density of nanowires for all observed specimens is about 10^{10} wires/cm^2.

The main advantage of this approach is the precise control of oxidizer and fuel dimensions at nanoscale. The method avoids both the incorporation of impurities and the oxidation of the Al at the fuel-oxidizer interface prior to ignition.

E. Molecular Engineering or "Bottom-Up" Approaches

Molecular engineering has been investigated very recently by only a few teams to control the fuel/oxidizer interfacial contact area and improve the homogeneity of the final material.

One interesting technique is the molecular self-assembly. It means that the fuel nanoparticles will arrange by themselves or enhanced by external forces, in a controlled manner around the oxidizers or vice versa. Fuel or oxidizer molecules can be arranged in inorganic solution or manipulated by using a polymer. Kim and Zachariah [79] presented a method to synthesize MIC in which the Al and Fe_2O_3 self-assembly is controlled by the electrostatic forces which exist between charged aerosol particles. The authors compared the reactivity of resulting Al/Fe_2O_3 with a randomly assembled Al/Fe_2O_3. As shown in Fig. 14(b), the nano-Al particles surround perfectly the surface of Fe_2O_3 particles and the contact between Al and

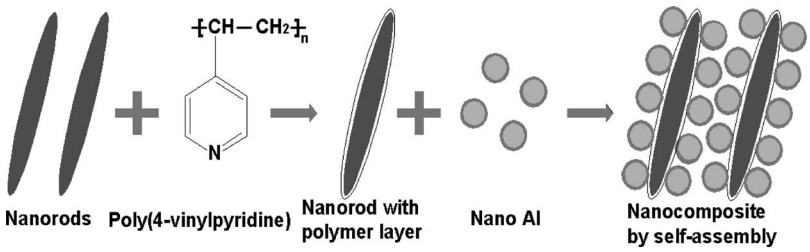

Fig. 15. Schematic of nano-Al self-assembly around CuO nanorods. Reproduced with permission from [80]. Copyright 2006 Materials Research Society.

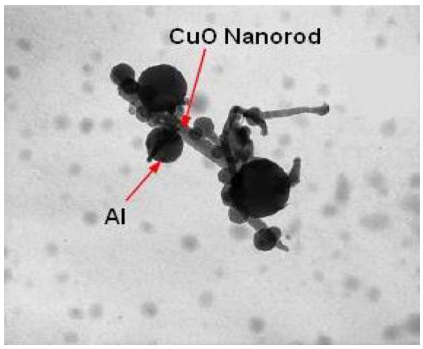

Fig. 16. TEM image of nano-Al assembly around CuO nanorods. Reproduced with permission from [80]. Copyright 2006 Materials Research Society.

Fe_2O_3 is intimate. Fig. 14(a) is a TEM image of nano Al/Fe_2O_3 synthesized by random Brownian assembly. It can be seen that nano-Al particles form linear chains in contact with the Fe_2O_3 particles. The authors' results showed that Al/Fe_2O_3 MIC materials electrostatically assembled are more powerful than those produced via random assembly due certainly to the enhanced fuel/oxidizer interfacial surface. The total measured heat of reaction is 1.8 kJ/g against 0.7 kJ/g for a random assembly that remains lower than the theoretical heat of reaction of Al/Fe_2O_3 MIC (3.9 kJ/g).

Subramaniam *et al.* [80] employed a polymer chain on which the nanoparticles (CuO and Al) are binded, as shown schematically in Fig. 15. The polymer is therefore a structural link for the nanoparticles assembly process. In a typical process, CuO nanorods are first prepared from a chemical route (by surfactant templating method). Then, the CuO nanorods are coated with the poly(4-vinyl pyridine) polymer from Aldrich in a sonic bath. After that, the CuO nanorods are removed from the solution, washed, dried, and mixed with nano-Al particles (80 nm in diameter with 2 nm of passivation layer). The resulting Al/CuO MIC is shown in Fig. 16. The highest burning rate measured by the authors is 2000 m/s for Al/CuO MIC synthesized by the polymer-based nano-self-assembly.

LAAS–Centre National de la Recherche Scientifique and CIRIMAT are exploring an innovative approach to realizing MIC directly on silicon making it very easy to integrate MIC into MEMS devices. First, metal oxide foam is achieved by self-assembly of primary individual metal-oxide nanoparticles onto silicon substrate. The self-assembly results in nanopores inside the metal oxide foam. Then, nano-Al is deposited inside the nanopores so as to have an intimate contact between Al and metal oxide.

V. Conclusion

The R&D of nano-EMs is a quite young field but is very active, and promising results could lead to interesting breakthrough in the field of microenergetic devices. For years, different synthesis approaches to enhance the performances of EMs and make them applicable to microscopic systems have been investigated and reported in this review.

The first approach consists of doping traditional EMs (HTBP, PETN, RDX, ...) with nanoparticles of Al and, more recently, CNT. The results are quite interesting but suffer from two main disadvantages. Besides the difficulty to get a final homogeneous mixture, the procedure of elaboration can be hazardous, and the finally obtained material has to be manipulated and reported on the initiator which is, if possible, very difficult.

The second approach widely investigated consists of elaborating MICs that exhibit very powerful reaction mainly because of its high redox capability and high thermal diffusivity. Different nano-based processes have been investigated to reduce the diffusion distances between reactant species and increase the surface-over-volume ratio. These MICs can be synthesized in different ways.

Powder mixing is a widely used method but not really applicable to microenergetic applications. Sol–gel is an interesting approach mainly because it presents process advantages in terms of homogeneity, cost, and safety. Fabrication of the nano-PSi-based EM is also very innovative and promising because it is totally integratable into standard semiconductor technologies. In particular, the nano-PSi-based EMs can be easily integrated on a silicon chip.

Modern technologies as nanopatterning provide nice opportunities to get a new class of tailored EMs. The elaboration of energetic multilayer nanofoils from PVD or sputtering is also a promising approach for the integration of nano-EMs within microsystems because of the compatibility with mass production process, the good quality of the fabricated layer, and the possibility to control precisely each metal and oxide thickness layer and interdiffusion region. More recently, a couple of "bottom-up" approaches have been investigated and seem to provide a good means to better understand the structural mechanisms governing the EMs thermal and dynamic properties. This "bottom-up" route would enable molecularly manipulated energetic substances and formulations having tailored chemical and physical properties, high performance, low sensitivity, and multifunctional capabilities [16], [21], [81]. This is a good route to access to a fundamental understanding of the evolution of the EMs properties with the size and intimacy of the constituents.

Although there has been considerable success in formulating new MIC with enhanced energy-release rates, the subject of achieving a precise control over the reactivity of nEMs is an opportunity for further research. To achieve a better understanding of nEMs properties, progress in computational method and tools is requested to assess the reactivity to predict the stability of these new classes of nEMs. Fundamental computations aimed toward the simulation of the behavior of nEMs are in the primary stage.

REFERENCES

[1] C. Rossi, D. Briand, M. Dumonteuil, T. Camps, P. Q. Pham, and N. F. de Rooij, "Matrix of 10 × 10 addressed solid propellant microthrusters: Review of the technologies," *Sens. Actuators A, Phys.*, vol. 126, no. 1, pp. 241–252, Jan. 2006.

[2] D. W. Youngner, S. T. Lu, E. Choueiri, J. B. Neidert, R. E. Black, III, K. J. Graham, D. Fahey, R. Lucus, and X. Zhu, "MEMS mega-pixel micro-thruster arrays for small satellite stationkeeping," presented at the 14th Annu. AIAA/USU Conf. Small Satellites, Logan, UT, Aug. 21–24, 2000, AIAA Paper SSC00-X-2.

[3] D. H. Lewis, Jr., S. W. Janson, R. B. Cohen, and E. K. Antonsson, "Digital micropropulsion," *Sens. Actuators A, Phys.*, vol. 80, no. 2, pp. 143–154, Mar. 2000.

[4] D. Teasdale, V. Milanovic, P. Chang, and K. Pister, "Microrockets for smart dust," *Smart Mater. Struc.*, vol. 10, no. 6, pp. 1145–1155, 2001.

[5] W. Lindsay, D. Teasdale, V. Milanovic, K. Pister, and C. F. Pello, "Thrust and electrical power from solid propellant microrockets," in *Proc. Tech. Dig. 14th IEEE Int. Conf. MEMS*, Piscataway, NJ, 2001, pp. 606–610.

[6] K. Takahashi, H. Ebisuzaki, H. Kajiwara, T. Achiwa, and K. Nagayama, "Design and testing of mega-bit microthruster arrays," presented at the Nanotech, Houston, TX, Sep. 9–12, 2002, Paper AIAA 2002-5758.

[7] S. Tanaka, R. Hosokawa, S. Tokudome, K. Hori, H. Saito, M. Watanabe, and M. Esashi, "MEMS-based solid propellant rocket array thruster with electrical feedthroughs," *Trans. Jpn. Soc. Aeronaut. Space Sci.*, vol. 46, no. 151, pp. 47–51, 2003.

[8] P. Q. Pham, D. Briand, C. Rossi, and N. F. De Rooij, "Downscaling of solid propellant pyrotechnical microsystems," in *Proc. 12th Int. Conf. Solid-State Sensors and Actuators (Transducers)*, Boston, MA, Jun. 8–12, 2003, pp. 1423–1426.

[9] Y. Zhao, B. A. English, Y. Choi, H. DiBiaso, G. Yuan, and M. G. Allen, "Polymeric microcombustors for solid-phase conductive fuels," in *Proc. 17th IEEE Int. Conf. MEMS*, Maastricht, The Netherlands, Jan. 25–29, 2004, pp. 498–501.

[10] K. L. Zhang, S. K. Chou, S. S. Ang, and X. S. Tang, "A MEMS-based solid propellant microthruster with Au/Ti igniter," *Sens. Actuators A, Phys.*, vol. 122, no. 1, pp. 113–123, Jul. 2005.

[11] T. Troianello, "Precision foil resistors used as electro-pyrotechnic initiators," in *Proc. 1st Electron. Compon. and Technol. Conf.*, Orlando, FL, May 29–Jun. 1, 2001, pp. 1413–1417.

[12] H. DiBiaso, B. A. English, and M. G. Allen, "Solid-phase conductive fuels for chemical microactuators," *Sens. Actuators A, Phys.*, vol. 111, no. 2/3, pp. 260–266, Mar. 2004.

[13] H. Laucht, H. Bartuch, and D. Kovalev, "Silicon initiator, from the idea to functional tests," in *Proc. 7th Int. Symp. and Exhib. Sophisticated Car Occupant Safety Syst.*, 2004, pp. 12–16.

[14] A. Hofmann, H. Laucht, D. Kovalev, V. Y. Timoshenko, J. Diener, N. Kunzner, and E. Gross, "Explosive composition and its use," U.S. Patent 6 984 274, Jan. 10, 2006.

[15] T. W. Barbee, R. L. Simpson, A. E. Gash, and J. H. Satcher, "Nanolaminate-based ignitors," U.S. Patent WO 2005 016 850 A2, Feb. 24, 2005.

[16] J. C. Hinshaw, "Thermite compositions for use as gas generants," International Patent WO 95/04672, Aug. 8, 1995.

[17] C. Rossi and D. Estève, "Pyrotechnic micro actuators," in *Proc. 11th EUROSENSORS XI*, Varsovie, Pologne, 1997, vol. 2, pp. 771–774.

[18] C. Rossi, D. Estève, and C. Mingués, "Pyrotechnic actuator: A new generation of Si integrated actuator," *Sens. Actuators A, Phys.*, vol. 74, no. 1–3, pp. 211–215, Apr. 1999.

[19] C. C. Hong, S. Murugesan, G. Beaucage, J. W. Choi, and C. H. Ahn, "A functioning on-chip pressure generator using solid chemical propellant for disposable lab-on-a-chip," *Lab Chip*, vol. 3, no. 4, pp. 281–286, 2003.

[20] A. A. Norton and M. A. Minor, "Pneumatic microactuator powered by the deflagration of sodium azide," *J. Microelectromech. Syst.*, vol. 15, no. 2, pp. 344–354, Apr. 2006.

[21] D. Li, X. B. Lu, Z. Z. Zhou, M. X. Qiu, and C. G. Lin, "Laser-initiated aluminothermic reaction applied to preparing Mo–Si film on silicon substrates," in *Proc. Mater. Res. Soc. Symp.*, 1988, vol. 101, pp. 487–490.

[22] "Pile àgrave; combustible pour l'alimentation d'appareils électroniques, notamment portables," Patent FR2 818 808, 2005. (in French).

[23] O. Vasylkiv and Y. Sakka, "Nanoexplosion synthesis of multimetal oxide ceramic nanopowders," *Nano Lett.*, vol. 5, no. 12, pp. 2598–2604, Dec. 2005.

[24] O. Vasylkiv, Y. Sakka, and V. V. Skorokhod, "Nano-blast synthesis of nano-size CeO2-Gd2O3 powders," *J. Amer. Ceram. Soc.*, vol. 89, no. 6, pp. 1822–1826, Jun. 2006.

[25] D. S. Stewart, "Miniaturization of explosive technology and microdetonics," in *Proc. 21st ICTAM*, Varsaw, Poland, Aug. 15–21, 2004.

[26] P. Pennarun, C. Rossi, D. Estève, and D. Bourrier, "Design, fabrication and characterization of a MEMS safe pyrotechnical igniter integrating arming, disarming and sterilization functions," *J. Micromech. Microeng.*, vol. 16, no. 1, pp. 92–100, Jan. 2006.

[27] A. S. Tappan, G. T. Long, A. M. Renlund, and S. H. Kravitz, "Microenergetic materials-microscale energetic material processing and testing," presented at the 41st AIAA Aerospace Sciences Meeting and Exhibit, Reno, NV, Jan. 6–9, 2003, Paper AIAA-2003-0242.

[28] A. S. Tappan, G. T. Long, B. Wroblewski, J. Nogan, H. A. Palmer, S. H. Kravitz, and A. M. Renlund, "Patterning of regular porosity in PETN microenergetic material thin films," in *Proc. 36th Int. Conf. ICT*, Karlsruhe, Germany, Jun. 28–Jul. 1, 2005, pp. 134–135.

[29] L. E. Fried, M. R. Manaa, P. F. Pagoria, and R. L. Simpson, "Design and synthesis of energetic materials," *Annu. Rev. Mater. Res.*, vol. 31, no. 1, pp. 291–321, 2001.

[30] C. Rossi and D. Esteve, "Micropyrotechnics, a new technology for making energetic microsystems: Review and prospective," *Sens. Actuators A, Phys.*, vol. 120, no. 2, pp. 297–310, May 2005.

[31] C. Rossi, B. Larangot, D. Lagrange, and A. Chaalane, "Final characterizations of MEMS-based pyrotechnical microthrusters," *Sens. Actuators A, Phys.*, vol. 121, no. 2, pp. 508–514, Jun. 2005.

[32] R. A. Rugunanan and M. E. Brown, "Combustion of binary and ternary silicon/oxidant pyrotechnic systems, Part I: Binary systems with Fe_2O_3 and SnO_2 as oxidants," *Combust. Sci. Technol.*, vol. 95, no. 1–6, pp. 61–83, 1994.

[33] C. E. Aumann, G. L. Skofronick, and J. A. Martin, "Oxidation behavior of aluminum nanopowders," *J. Vac. Sci. Technol. B, Microelectron. Process. Phenom.*, vol. 13, no. 2, pp. 1178–1183, May 1995.

[34] M. E. Brown, S. J. Taylor, and M. J. Tribelhorn, "Fuel-oxidant particle contact in binary pyrotechnic reactions," *Propellants Explos. Pyrotech.*, vol. 23, no. 6, pp. 320–327, 1998.

[35] J. Zhi, L. S. Fen, Z. F. Qi, L. Z. Ru, Y. C. Mei, L. Yang, and L. S. Wen, "Research on the combustion properties of propellants with low content of nano metal powders," *Propellants Explos. Pyrotech.*, vol. 31, no. 2, pp. 139–147, 2006.

[36] K. Park, D. Lee, A. Rai, D. Mukherjee, and M. R. Zachariah, "Size-resolved kinetic measurements of aluminum nanoparticle oxidation with single particle mass spectrometry," *J. Phys. Chem., B*, vol. 109, no. 15, pp. 7290–7299, Apr. 2005.

[37] G. V. Ivanov and F. Tepper, "Activated aluminium as a stored energy source for propellants," in *Proc. 4th Int. Symp. Spec. Topics Chem. Propulsion*, Stockholm, Sweden, May 27–28, 1996, pp. 636–644.

[38] M. J. Chiaverini, N. Serin, D. K. Johnson, Y. C. Lu, and K. K. Kuo, "Challenges," in *Propellants and Combustion 100 Years After Nobel*, K. K. Kuo *et al.*, Ed. New York: Begell House, 1997, pp. 719–733.

[39] R. W. Armstrong, B. Baschung, D. W. Booth, and M. Samirant, "Enhanced propellant combustion with nanoparticles," *Nano Lett.*, vol. 3, no. 2, pp. 253–255, 2003.

[40] V. N. Simonenko and V. E. Zarko, "Comparative studying of the combustion behavior of composite propellant containing ultrafine aluminum," in *Proc. 30th Int. Annu. Conf. ICT*, Karlsruhe, Germany, Jun. 29–Jul. 2, 1999, p. 21/1.

[41] M. M. Mench, C. L. Yeh, and K. K. Kuo, "Propellant burning rate enhancement and thermal behavior of ultra-fine aluminum powders (Alex)," in *Proc. 29th Int. Annu. Conf. ICT*, Karlsruhe, Germany, Jun. 30–Jul. 3, 1998, p. 30/1.

[42] S. K. Poehlein, D. Burch, R. Johnson, M. Beyard, and S. Larson, "Requalification of demilitarized HMX for military use," in *Proc. 36th Int. Annu. Conf. ICT & 32nd Int. Pyrotechnics Seminar*, Karlsruhe, Germany, Jun. 28–Jul. 1, 2005, pp. 31–33.

[43] A. Pivkina, P. Ulyanova, Y. Frolov, S. Zavyalov, and J. Schoonman, "Nanomaterials for heterogeneous combustion," *Propellants Explos. Pyrotech.*, vol. 29, no. 1, pp. 39–48, 2004.

[44] M. R. Manaa, A. R. Mitchell, R. G. Garza, P. F. Pagoria, and B. E. Watkins, "Flash ignition and initiation of explosives-nanotubes mixture," *J. Amer. Chem. Soc.*, vol. 127, no. 40, pp. 13 786–13 787, Oct. 2005.
[45] Y. Frolov, A. Pivkina, P. Ulyanova, and S. Zavyalov, "Nanomaterials and nanostructures as components for high-energy condensed systems," in *Proc. 28th Int. Pyrotechnics Seminar*, Adelaide, Australia, Nov. 2001, p. 305.
[46] L. L. Wang, Z. A. Munir, and Y. M. Maximov, "Thermite reactions: Their utilization in the synthesis and processing of materials," *J. Mater. Sci.*, vol. 28, no. 14, pp. 3693–3708, 1993.
[47] B. S. Bockmon, M. L. Pantoya, S. F. Son, B. W. Asay, and J. T. Mang, "Combustion velocities and propagation mechanisms of metastable interstitial composites," *J. Appl. Phys.*, vol. 98, no. 6, pp. 064 903/1–064 903/7, Sep. 2005.
[48] J. J. Granier and M. L. Pantoya, "Laser ignition of nanocomposite thermites," *Combust. Flame*, vol. 138, no. 4, pp. 373–383, 2004.
[49] M. L. Pantoya and J. J. Granier, "Combustion behavior of highly energetic thermites: Nano versus micron composites," *Propellants Explos. Pyrotech.*, vol. 30, no. 1, pp. 53–62, 2005.
[50] J. Sun, M. L. Pantoya, and S. L. Simon, "Dependence of size and size distribution on reactivity of aluminum nanoparticles in reactions with oxygen and MoO_3," *Thermochim. Acta*, vol. 444, no. 2, pp. 117–127, 2006.
[51] S. Bhattacharya, Y. Gao, S. Apperson, S. Subramaniam, R. Shende, S. Gangopadhyay, and E. Talantsev, "A novel on-chip diagnostic method to measure burn rates of energetic materials," *J. Energ. Mater.*, vol. 24, no. 1, pp. 1–15, Jan.–Mar. 2006.
[52] S. H. Fischer and M. C. Grubelich, "Theoretical energy release of thermites, intermetallics, combustible metals," in *Proc. 24th Int. Pyrotechnics Seminar*, Monterey, CA, Jul. 1998, pp. 1–6.
[53] *COACH: COmputer Aided CHemistry*, Saint Martin d'Heres, France: Thermodata. [Online]. Available: http://thermodata.online.fr/coachang.html
[54] K. Moore and M. L. Pantoya, "Combustion of environmentally altered molybdenum trioxide nanocomposites," *Propellants Explos. Pyrotech.*, vol. 31, no. 3, pp. 182–187, 2006.
[55] A. Prakash, A. V. McCormick, and M. R. Zachariah, "Synthesis and reactivity of a super-reactive metastable intermolecular composite formulation of Al/$KMnO_4$," *Adv. Mater.*, vol. 17, no. 7, pp. 900–903, 2005.
[56] L. Duraes, "Radial combustion propagation in Iron (III) oxide/aluminum thermite mixtures," *Propellants Explos. Pyrotech.*, vol. 31, no. 1, pp. 42–49, 2006.
[57] A. E. Gash, T. M. Tillotson, J. H. Satcher, Jr., J. F. Poco, L. W. Hrubesh, and R. L. Simpson, "Use of epoxides in the sol–gel synthesis of porous Iron(III) oxide monoliths from Fe(III) salts," *Chem. Mater.*, vol. 13, no. 3, pp. 999–1007, 2001.
[58] T. M. Tillotson, A. E. Gash, R. L. Simpson, L. W. Hrubesh, J. H. Satcher, Jr., and J. F. Poco, "Nanostructured energetic materials using sol–gel methodologies," *J. Non-Cryst. Solids*, vol. 285, no. 1, pp. 338–345, Jun. 2001.
[59] A. W. Miziolek, "Nanoenergetics: An emerging technology area of national importance," *AMPTIAC*, vol. 6, no. 1, pp. 43–48, 2002.
[60] A. E. Gash, T. M. Tillotson, J. H. Satcher, Jr., L. W. Hrubesh, and R. L. Simpson, "New sol–gel synthetic route to transition and main-group metal oxide aerogels using inorganic salt precursors," *J. Non-Cryst. Solids*, vol. 285, no. 1, pp. 22–28, Jun. 2001.
[61] A. Prakash, A. V. McCormick, and M. R. Zachariah, "Aero-sol–gel synthesis of nanoporous iron-oxide particles: A potential oxidizer for nanoenergetic materials," *Chem. Mater.*, vol. 16, no. 8, pp. 1466–1471, 2004.
[62] D. Prentice, M. L. Pantoya, and B. J. Clapsaddle, "Effect of nanocomposite synthesis on the combustion performance of a ternary thermite," *J. Phys. Chem., B*, vol. 109, no. 43, pp. 20 180–20 185, 2005.
[63] B. J. Clapsaddle, D. W. Sprehn, A. E. Gash, J. H. Satcher, Jr., and R. L. Simpson, "A versatile sol–gel synthesis route to metal-silicon mixed oxide nanocomposites that contain metal oxides as the major phase," *J. Non-Cryst. Solids*, vol. 350, no. 1, pp. 173–181, 2004.
[64] A. Prakash, A. V. McCormick, and M. R. Zachariah, "Tuning the reactivity of energetic nanoparticles by creation of a core-shell nanostructure," *Nano Lett.*, vol. 5, no. 7, pp. 1357–1360, Jul. 2005.
[65] T. A. Vine, S. Tinston, and R. Fairhutst, "Application of physical vapor deposition to the manufacture of pyrotechnics," in *Proc. 28th Int. Pyrotechnics Seminar*, Adelaide, Australia, Nov. 4–9, 2001, p. 725.
[66] K. J. Blobaum, M. E. Reiss, J. M. P. Lawrence, and T. P. Weihs, "Deposition and characterization of a self-propagating CuOx/Al thermite reaction in a multilayer foil geometry," *J. Appl. Phys.*, vol. 94, no. 5, pp. 2915–2922, 2003.
[67] A. J. Gavens, D. V. Heerden, A. B. Mann, M. E. Reiss, and T. P. Weihsa, "Effect of intermixing on self-propagating exothermic reactions in Al/Ni nanolaminate foils," *J. Appl. Phys.*, vol. 87, no. 3, pp. 1255–1263, Feb. 2000.
[68] P. Tagststrom, P. Martensson, U. Jansson, and J. O. Carlsso, "Atomic layer epitaxy of tungsten oxide films using oxyfluorides as metal precursors," *J. Electrochem. Soc.*, vol. 146, no. 8, pp. 3139–3143, Aug. 1999.
[69] H. Seim, M. Niemminen, L. Niinisto, A. Kjekshus, and L. S. Johansson, "Growth of LaCoO3 thin film from beta-diketonate precursors," *Appl. Surf. Sci.*, vol. 112, no. 1, pp. 243–250, 1997.
[70] T. S. Yang, W. Cho, M. Kim, K. S. An, T. M. Chung, C. G. Kim, and Y. Kim, "Atomic layer deposition of nickel oxide films using $Ni(dmamp)_2$ and water," *J. Vac. Sci. Technol. A, Vac. Surf. Films*, vol. 23, no. 4, pp. 1238–1243, 2005.
[71] J. D. Ferguson, K. J. Buechler, A. W. Weimer, and S. M. George, "SnO_2 atomic layer deposition on ZrO_2 and Al nanoparticles: Pathway to enhanced thermite materials," *Powder Technol.*, vol. 156, no. 2/3, pp. 154–163, 2005.
[72] P. McCord, S. L. Yau, and A. J. Bard, "Chemiluminescence of anodized and etched silicon: Evidence for a luminescent siloxene-like layer on porous silicon," *Science*, vol. 257, no. 5066, p. 68, Jul. 1992.
[73] D. Kovalev, V. Y. Timoshenko, N. Künzner, E. Gross, and F. Koch, "Strong explosive interaction of hydrogenated porous silicon with oxygen at cryogenic temperatures," *Phys. Rev. Lett.*, vol. 87, no. 6, pp. 068 301/1–068 301/4, Aug. 2001.
[74] F. V. Mikulec, J. D. Kirtland, and M. J. Sailor, "Explosive nanocrystalline porous silicon and its use in atomic emission spectroscopy," *Adv. Mater.*, vol. 14, no. 1, pp. 38–41, Jan. 2002.
[75] X. Li and P. W. Bohna, "A metal-assisted chemical etching in HF/H_2O_2 produces porous silicon," *Appl. Phys. Lett.*, vol. 77, no. 6, pp. 2572–2574, 2000.
[76] L. Menon, S. Patibandla, K. Bhargava Ram, S. I. Shkuratov, D. Aurongzeb, M. Holtz, J. Berg, J. Yun, and H. Temkin, "Ignition studies of Al/Fe_2O_3 energetic nanocomposites," *Appl. Phys. Lett.*, vol. 84, no. 23, pp. 4737–4737, 2004.
[77] H. Masuda and K. Fukuda, "Ordered metal nanohole arrays made by a two-step replication of honeycomb structures of anodic alumina," *Science*, vol. 268, no. 5216, pp. 1466–1468, Jun. 1995.
[78] H. Masuda, H. Yamada, M. Satoh, H. Asoh, M. Nakao, and T. Tamamura, "Highly ordered nanochannel-array architecture in anodic alumina," *Appl. Phys. Lett.*, vol. 71, no. 19, pp. 2770–2772, Nov. 1997.
[79] S. H. Kim and M. R. Zachariah, "Enhancing the rate of energy release from NanoEnergetic materials by electrostatically enhanced assembly," *Adv. Mater.*, vol. 16, no. 20, pp. 1821–1825, 2004.
[80] S. Subramaniam, S. Hasan, S. Bhattacharya, Y. Gao, S. Apperson, M. Hossain, R. V. Shende, S. Gangopadhyay, P. Redner, D. Kapoor, and S. Nicolich, "Self-assembled nanoenergetic composite," in *Proc. Mater. Res. Soc. Symp.*, 2006, vol. 896, pp. 0896-H01-05.1–0896-H01-05.6.
[81] V. Sundaram, K. V. Logan, and R. F. Speyer, "Aluminothermic reaction path in the synthesis of a $TiB_2-Al_2O_3$ composite," *J. Mater. Res.*, vol. 12, no. 7, pp. 1681–1684, Jul. 1997.

Carole Rossi received the degree in engineering from the National Institute of Applied Science, Toulouse, France, in 1994 and the Ph.D. degree in electrical engineering and physics in 1997.

She is currently a Researcher at the French National Center for Scientific Research (CNRS), Toulouse, where she is a Member of the Microsystems and Systems Integration (MIS) Group, Laboratoire d'Analyse et d'Architecture des Systèmes, in the MEMS department. Her research interests include microenergetic for MEMS, micropyrotechnical systems, and power MEMS for electrical generation. She is currently leading the power MEMS research area at LAAS, and her team proposes new concepts for actuation and energy on a chip.

Kaili Zhang received the B.S. degree in mechanical engineering from Dong Hua University, China, in 1997 and the Ph.D. degree in microsystems from the National University of Singapore, Kent Ridge, Singapore, in 2005.

From 2005 to 2006, he was with the National University of Singapore as a Postdoctoral Research Fellow. He is currently with the Microsystems and Systems Integration (MIS) Group, Laboratoire d'Analyse et d'Architecture des Systèmes (LAAS), French National Center of Scientific Research (CNRS). His current research interests include nanoenergetic materials, nanometal oxides, nanocatalysis, micropropulsion, and thin films.

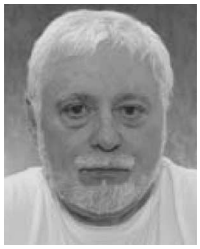

Daniel Estève was born in 1941. He received the Ph.D. degree in 1966 and the Doctorat d'Etat degree in 1972.

He joined the French National Center of Scientific Research (CNRS) in 1966, where he is currently the Director of Research and a member of the Microsystems and Systems Integration (MIS) Group, Laboratoire d'Analyse et d'Architecture des Systèmes (LAAS). He was one of the first members of the LAAS-CNRS, which was founded in 1968. During 1982-1986, he was the Director of LAAS-CNRS. He has been with LAAS since the beginning of microsystems activities there. His fields of interest have covered a wide range from electronic circuit and electronic device modeling to microsystems modeling and simulation, design, and characterization.

Pierre Alphonse received the Ph.D. degree from University of Toulouse, Toulouse, France, in 1986.

He is currently a Research Engineer at the Centre Interuniversitaire de Recherche et d'Ingénierie des Matériaux (CIRIMAT), Toulouse. His research interests include the design and analysis of materials for catalysis, especially in the field of pollution control and energy conversion.

Philippe Tailhades was born on July 19, 1960, at Mazamet, France. He received the Ph.D. degree in Material Science in 1988 and the Habilitation à Diriger les Recherches in 1994.

He is currently the Vice Director of the Centre Interuniversitaire de Recherche et d'Ingénierie des Matériaux (CIRIMAT), Toulouse, France. His research interests include the preparation of original metallic oxides, especially spinel ferrites, in the form of fine powders, thin films, or bulk ceramics and the study of the magnetic, electric, and optical properties of these materials. He also works on the preparation of special metallic powders.

Dr. Tailhades received the silver medal of CNRS in France in 2000.

Constantin Vahlas received the Bachelor's degree in chemical engineering from the National Technical University of Athens, Athens, Greece, and the Master's degree and the doctoral degree in metallurgy from the National Polytechnic Institute of Grenoble, Grenoble, France.

He is currently the National Center for Scientific Research (CNRS) Director of Research at the Centre Interuniversitaire de Recherche et d'Ingénierie des Matériaux (CIRIMAT), Toulouse, France, where he is the Head of the Chemical Vapor Deposition Group. He is the Director of a European Integrated Laboratory on Advanced Coating Technologies in the frame of the Network of Excellence on Complex Metallic Alloys. He has been working with CNRS for 21 years, where his early studies centered on thermochemistry of the gas-solid processes and on CVD of ceramic and pyrolytic carbon films for microelectronics and composite materials applications.